Parallel Flow Through Ordered Fibers: An Analytical Approach

A. Tamayol[1]
e-mail: ali_tamayol@sfu.ca

M. Bahrami
e-mail: mbahrami@sfu.ca

Mechatronic Systems Engineering,
School of Engineering Science,
Simon Fraser University,
BC, V3T0A3, Canada

In this study, fully developed flow parallel to ordered fibers is investigated analytically. The considered fibrous media are made up of in-line (square), staggered, and hexagonal arrays of cylinders. Starting from the general solution of Poisson's equation, compact analytical solutions are proposed for both velocity distribution and permeability of the considered structures. In addition, independent numerical simulations are performed for the considered arrangements over the entire range of porosity and the results are compared with the proposed solutions. The developed solutions are successfully verified through comparison with experimental data, collected by others, and the present numerical results over a wide range of porosity. The results show that for the ordered arrangements with high porosity, the parallel permeability is independent of the microstructure geometrical arrangements; on the other hand, for lower porosities the hexagonal arrangement provides lower pressure drop, as expected.
[DOI: 10.1115/1.4002169]

Keywords: creeping flow, parallel permeability, ordered fibers, analytical solution, fibrous porous media

1 Introduction

Transport phenomena in porous media have been the focus of numerous studies since the 1850s, which indicates the importance of this topic. Most of these studies refer to granular materials with low and medium porosities, $0.3<\varepsilon<0.6$ [1]. Fibrous structures, made up of cylindrical-like particles, can form mechanically stable geometries with high porosity, up to 0.99 [2]. Moreover, these fibrous structures feature low-weight, high surface-to-volume ratios, and high heat transfer coefficients [3], which make them suitable for application in several engineering areas including: filtration and separation of particles [4,5], composite fabrication [6,7], heat exchangers [3], and fuel cells [8]. Experimental observations have shown that a linear relationship exists between the volume-averaged superficial fluid velocity and the pressure gradient; this is called Darcy's law [1].

$$-\frac{dP}{dz}=\frac{\mu}{K}U_D \tag{1}$$

where μ is the fluid viscosity and K is the viscous permeability of the medium. Viscous permeability can be interpreted as the ability of the porous matrix to pass fluids. Macroscopic transport properties such as permeability and heat transfer coefficient are functions of geometrical features of the porous medium; thus, determination of exact transport properties for real fibrous materials with random structures is very complex and in many cases not possible. However, several researchers have argued that unidirectional fibers are the most permeable fibrous structures when flow is parallel to the fibers axes [9]. Moreover, a blend of normal and parallel permeabilities of unidirectional arrangements provides an estimate for the permeability of random fibrous media, e.g., Jackson and James [10] and Happel and Brenner [11]. Therefore, a detailed analysis of parallel permeability of unidirectional fibers is valuable.

Happel [12] and Sparrow and Loeffler [13] studied parallel permeability for unidirectional cylinders for heat exchanger application. Happel [12] assumed a circular unit cell with a single cylinder located at its center and applied zero-shear stress boundary condition on the outer surface of the control volume; this method is called the limited boundary layer approach. However, the model of Ref. [12] cannot accurately predict the parallel permeability for lower porosities where neighboring fibers play an important role [10].

Sparrow and Loeffler [13], on the other hand, considered both square and staggered arrangements of monodispersed fibers. They used the general solution of Poisson's equation in the cylindrical coordinate system and applied the boundary conditions at finite discrete points. The evaluated coefficients in their series solution were functions of porosity; therefore, they proposed an approximate compact relationship, which was reported to be accurate for highly porous structures, i.e., $\varepsilon>0.9$ [13]. The approximate model of Sparrow and Loeffler [13], for staggered arrangement, was identical to the model of Happel [12]. Velocity distribution was also reported in a tabular form, which was not easy-to-use. Later, Drummond and Tahir [14] performed a comprehensive analytical investigation of normal and parallel flows for various ordered arrays of fibers. For parallel flow, they started from the general solution of Poisson's equation in the form of a series. Drummond and Tahir [14] claimed that their singularity method was more accurate than the approach of Sparrow and Loeffler [13]. However, the models of Drummond and Tahir [14] for normal flow were not accurate [15]. Drummond and Tahir [14] did not report explicit relationships for the velocity distribution.

Wang [16] studied normal and parallel flow through rectangular arrays of fibers using the eigenfunction expansion and collocation method. However, Wang [16] did not provide a compact relationship for velocity distribution and the accuracy of the model for permeability was limited to high porosity structures. Recently, Tamayol and Bahrami [17], assuming a parabolic velocity distribution and using an integral technique, determined the normal and parallel permeabilities of square arrays of cylinders. In a subsequent work, Tamayol and Bahrami [18] performed a comprehensive numerical study and reported the normal and the parallel permeability of square fiber arrangements over a wide range of porosity. Comparison of the numerical results with their analytical relationship showed that although their model could capture the trends of numerical results, the differences were significant in the medium range of porosity $0.5<\varepsilon<0.8$ [18]. Comparing the numerical velocity distribution with the parabolic profile, Tamayol and Bahrami [17] argued that the assumption of parabolic velocity distribution was not accurate. Therefore, the objectives of the present study are as follows:

(1) to develop velocity profiles for parallel flow toward ordered arrays of fibers
(2) to find compact and accurate models for parallel permeability in unidirectional fibrous matrices
(3) to verify the analyses through comparison with experimental and numerical data

In this study, porous material is assumed to be periodic and is represented by a three-dimensional unit cell. The point matching technique originally developed by Sparrow and Loeffler [13] for

[1]Corresponding author.

Contributed by the Fluids Engineering Division of ASME for publication in the JOURNAL OF FLUIDS ENGINEERING. Manuscript received November 21, 2009; final manuscript received July 11, 2010; published online November 3, 2010. Assoc. Editor: Mark Stremler.

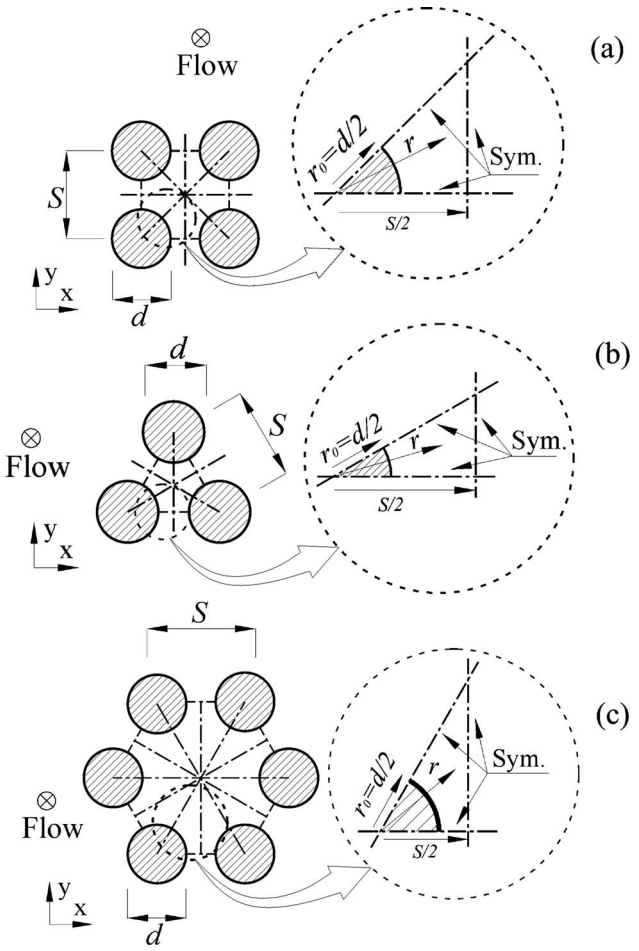

Fig. 1 Unit cell for (*a*) square, (*b*) staggered, and (*c*) hexagonal arrangements

staggered and square fiber arrays is followed here and extended to hexagonal fibers arrangement to find analytical solutions for velocity distribution. The solution is then used to report novel, compact, and accurate models for velocity distribution in ordered fibers arrangements. The reported models for velocity distribution are a powerful tool for finding other transport properties of the considered fibrous media such as heat and mass transfer coefficients. Employing an integral technique, the proposed relationships for velocity distribution are used to develop compact models for parallel permeability in the considered geometries. Due to a lack of experimental and numerical data for parallel flow in unidirectional arrangements, numerical simulations are also performed using FLUENT software [19], over the entire range of porosity to validate the proposed models for velocity distribution and permeability.

2 Geometrical Modeling

Following the approach successfully used by others [20–26] a representative unit cell is considered to analyze the geometry of the fibrous media. The unit cell (or basic cell) is the smallest volume, which can represent characteristics of the whole microstructure. In the following subsections, various ordered arrangements, shown in Fig. 1, will be investigated.

Using geometric symmetry, only the selected regions of the unit cells are considered in the analysis. The solid volume fraction and porosity of square, staggered, and hexagonal arrays are

$$\varphi = 1 - \varepsilon = \begin{cases} \dfrac{\pi d^2}{4S^2} & \text{square} \\ \dfrac{\pi d^2}{2\sqrt{3}S^2} & \text{staggered} \\ \dfrac{\pi d^2}{3\sqrt{3}S^2} & \text{hexagonal} \end{cases} \tag{2}$$

Therefore, the minimum possible values of ε for square, staggered, and hexagonal arrangements with no overlapping are 0.215, 0.094, and 0.395, respectively. These values indicate the touching limit of fibers.

3 Velocity Distribution

Laminar, steady, and fully developed flow parallel to square, staggered, and hexagonal fiber arrangements, shown in Fig. 1, is investigated. Darcy's relationship, Eq. (1), holds when the flow passing through pores is in creeping regime, i.e., inertial effects are negligible [1]. In the fully developed parallel flow, the velocity vector has only one nonzero component, which is in the lengthwise direction. As such, the following analyses are valid for the entire range of laminar flows. Applying the abovementioned assumptions, the conservation of linear momentum leads to Poisson's equation

$$\frac{\partial^2 w}{\partial r^2} + \frac{\partial w}{r\,\partial r} + \frac{\partial^2 w}{r^2\,\partial\,\theta^2} = \frac{1}{\mu}\left(\frac{dP}{dz}\right) \tag{3}$$

where w is the velocity component in the z-direction. The general solution of this equation is [27]

$$w = A + B\ln r + \frac{r^2}{4\mu}\left(\frac{dP}{dz}\right) + \sum_{k=1}^{\infty}(C_k r^k + D_k r^{-k})(E_k \cos k\theta + F_k \sin k\theta) \tag{4}$$

For square arrangement, symmetry lines are located at $\theta=0$ and $\theta=\pi/4$. The first condition results in $F_k=0$ and the second condition holds when $k=4,8,12,\ldots$. The no-slip boundary condition on the solid walls leads to

$$D_k = C_k r_0^{2k} \quad \text{and} \quad A = -B\ln r_0 - \frac{r_0^2}{4\mu}\left(\frac{dP}{dz}\right) \tag{5}$$

Total frictional force exerted on the fluid by solid rods must be balanced by the net pressure force acting over the entire cross-section of the basic cell.

$$\int_0^{\pi/4} \mu\left(\frac{\partial w}{\partial r}\right)_{r=r_0} r_0 d\theta = \int_0^{\pi/4}\int_{r_0}^{S/2\cos\theta}\left(\frac{dP}{dz}\right) r dr d\theta \tag{6}$$

Solving for Eq. (6), the constant B can be found

$$B = -\frac{S^2}{2\pi\mu}\left(\frac{dP}{dz}\right) \tag{7}$$

Consequently, the velocity distribution becomes

$$w^* = \left[\frac{2S^2}{\pi d^2}\ln\eta - \frac{\eta^2-1}{4} + \sum_{k=1}^{\infty}\frac{G_k d^{4k-2}}{2^{4k}S^{4k-2}}(\eta^{4k} - \eta^{-4k})\cos 4k\theta\right] \tag{8}$$

$$w^* = \frac{w}{-\dfrac{d^2}{4\mu}\left(\dfrac{dP}{dz}\right)}, \quad \eta = \frac{r}{d/2}$$

Table 1 Calculated coefficients in velocity distribution.

S/d	ε	g_1	g_2	g_3	g_4	g_5
Square arrangement						
4.0	0.95	−0.1253	−0.0106	−0.0006	0	0
2.0	0.80	−0.1250	−0.0105	−0.0006	0	0
1.5	0.65	−0.1225	−0.0091	−0.0002	0	0
1.2	0.45	−0.1104	−0.0024	−0.0015	0.0003	0
1.1	0.35	−0.0987	0.0036	0.0029	0.0005	0
1.05	0.29	−0.0904	0.0073	0.0032	0.0002	0
Staggered arrangement						
4.0	0.94	−0.0505	−0.0008	0.0000	0	0
2.0	0.77	−0. 0505	−0.0008	0.0000	0	0
1.5	0.60	−0. 0502	−0.0007	0.0001	0	0
1.2	0.37	−0. 0469	0.0007	0.0002	0.0000	0
1.1	0.25	−0.0416	0.0028	0.0004	0.0000	0
1.05	0.18	−0.0368	0.0043	0.0003	−0.0001	0.0000
Hexagonal arrangement						
4.0	0.96	−0.2850	−0.0365	−0.0048	−0.0006	−0.0001
2.0	0.85	−0.2827	−0.0350	−0.0043	−0.0005	0.0000
1.5	0.73	−0.2728	−0.0286	−0.0019	0.0002	0.0001
1.2	0.58	−0.2433	−0.0096	0.0053	0.0021	0.0006
1.1	0.50	−0.2216	0.0038	0.0093	0.0029	0.0004
1.05	0.45	−0.2076	0.0116	0.0103	0.0027	−0.0003

The last constant G_k is found by applying the symmetry condition on the unit cell border where $r=S/(2\cos\theta)$. Therefore, one can write

$$\frac{2}{\pi}(\cos\theta)^2-\frac{1}{2}+\sum_{k=1}^{\infty}\frac{g_k}{\cos\theta^{4k-1}}\left[\cos(4k-1)\theta+\left(\frac{d\cos\theta}{S}\right)^{8k}\cos(4k+1)\theta\right]=0 \tag{9}$$

where

$$g_k=G_k 4k\left(\frac{S}{2}\right)^{4k-2} \tag{10}$$

Sparrow and Loeffler [13] applied Eq. (9) at a finite number of points along the boundary and solved the resulting set of linear equations to determine the unknown coefficients, i.e., g_k. The same approach is followed here and the calculated coefficients for several porosities are listed in Table 1. The listed values are in agreement with the values reported by Sparrow and Loeffler [13].

The triangular unit cell section for the staggered fiber arrangements is shown in Fig. 1(*b*). The symmetry boundaries are located at $\theta=0$ and $\theta=\pi/6$. The governing equation and its general solution are still Eqs. (4) and (5). Following the same procedure used in the previous subsection and applying symmetry boundary conditions leads to

$$w^*=\left[\frac{\sqrt{3}S^2}{\pi d^2}\ln\eta-\frac{\eta^2-1}{4}+\sum_{k=1}^{\infty}\frac{g_k}{6k}\left(\frac{d}{S}\right)^{6k-2}(\eta^{6k}-\eta^{-6k})\cos 6k\theta\right] \tag{11}$$

The unknown coefficients are evaluated with the same approach used for square arrangements and the results as listed in Table 1.

Following the same approach and considering the location of the symmetry lines for hexagonal arrays at $\theta=0$ and $\theta=\pi/3$, the velocity distribution can be found as

$$w^*=\left[\frac{3\sqrt{3}S^2}{2\pi d^2}\ln\eta-\frac{\eta^2-1}{4}+\sum_{k=1}^{\infty}\frac{g_k}{3k}\left(\frac{d}{S}\right)^{3k-2}(\eta^{3k}-\eta^{-3k})\cos 3k\theta\right] \tag{12}$$

The unknown coefficients are listed in Table 1. From the listed coefficients in Table 1 and the form of the series solutions in Eqs. (8), (11), and (12), it is expected that truncating the series from the second term, does not affect the velocity distributions significantly. Our analysis also showed that substituting g_1 with an average value has a negligible impact on the predicted results (less than 4%). Therefore, g_1 is replaced by −0.107, −0.0437, and −0.246 for square, staggered, and hexagonal arrangements, respectively. Hence, the velocity distribution will be

$$w^*=\begin{cases}\left[\dfrac{2S^2}{\pi d^2}\ln\eta-\dfrac{\eta^2-1}{4}-\dfrac{0.0287d^2}{S^2}(\eta^4-\eta^{-4})\cos 4\theta\right] & \text{square}\\ \left[\dfrac{\sqrt{3}S^2}{\pi d^2}\ln\eta-\dfrac{\eta^2-1}{4}-\dfrac{0.007d^4}{S^4}(\eta^6-\eta^{-6})\cos 6\theta\right] & \text{staggered}\\ \left[\dfrac{3\sqrt{3}S^2}{2\pi d^2}\ln\eta-\dfrac{\eta^2-1}{4}-\dfrac{0.082d}{S}(\eta^3-\eta^{-3})\cos 3\theta\right] & \text{hexagonal}\end{cases} \tag{13}$$

Equation (13) is valid over the entire range of porosity for the considered geometries.

3.1 Numerical Simulations. Due to the lack of experimental and numerical data for parallel flow through ordered arrangements of fibers [15], a numerical study is performed using FLUENT software [19] to verify the solution. Structured grids are generated using Gambit [19], the preprocessor in the FLUENT [19] package; numerical grid aspect ratios are kept in the range of 1–5. FLUENT [19] is a finite volume based code and a second order upwind scheme is selected to discretize the governing equations. SIMPLE algorithm is employed for pressure-velocity coupling. The inlet velocity to the media is assumed to be uniform; this assumption allows one to study the developing length. To ensure that the fully developed condition is achieved, very long cylinders are considered, i.e., $L/d>40$; the fully developed section pressure drops are used for calculating the permeability. Constant pressure boundary condition is applied on the computational domain outlet. The symmetry boundary condition is applied on the side borders of the unit cells. Grid independence is tested for different cases and the size of the computational grids used for each geometry are selected such that the maximum difference in the predicted values for pressure gradient is less than 2%. The convergence criterion, i.e., the maximum relative error in the value of dependent variables between two successive iterations, is set at 10^{-6}.

To verify the proposed velocity distribution for the square arrangements, numerical and analytical velocity profiles are plotted in Figs. 2 and 3 for square and staggered arrangements. The velocity magnitudes are nondimensionalized using the volume-averaged velocity U_D. These figures indicate that Eq. (13) accurately predicts the velocity distribution in the considered geometries.

4 Permeability

Velocity distributions are developed analytically for parallel flow through square, staggered, and hexagonal arrays of cylinders in previous sections. Moreover, the flow-fields are solved numerically to verify the theoretical results. The volumetric flow rate that passes the medium is found by integrating Eq. (13) over the pore area. Substituting for dP/dz from Darcy's equation and using the solid volume fraction definitions for square arrangement of fibers, the nondimensional permeability is simplified as

$$K^* = \frac{K}{d^2} = \begin{cases} \frac{1}{16\varphi}\left[-1.479 - \ln\varphi + 2\varphi - \frac{\varphi^2}{2} - 0.0186\varphi^4\right] & \text{square} \\ \frac{1}{16\varphi}\left[-1.498 - \ln\varphi + 2\varphi - \frac{\varphi^2}{2} - 0.0018\varphi^6\right] & \text{staggered} \\ \frac{1}{16\varphi}\left[-1.352 - \ln\varphi + 2\varphi - \frac{\varphi^2}{2} - 0.246\varphi^3\right] & \text{hexagonal} \end{cases} \tag{14}$$

To verify the proposed model for parallel permeability of square arrays, Eq. (14), and numerical results are plotted in Fig. 4. In addition, experimental data of Sullivan [28] and Skartsis et al. [29] and the numerical results reported by Higdon and Ford [26] are included. Figure 4 shows that the present model is in agreement with the experimental and the numerical data. The maximum difference of the present model with numerical and experimental data is less than 8%. The present solution is compared with the analytical models of Happel [12] and Tamayol and Bahrami [17] in Fig. 5. As shown in Fig. 5, the present model accurately predicts the numerical results. More importantly, the present solution enables one to predict the velocity distribution in the unit cell. Although the model of Drummond and Tahir [14] is accurate, they

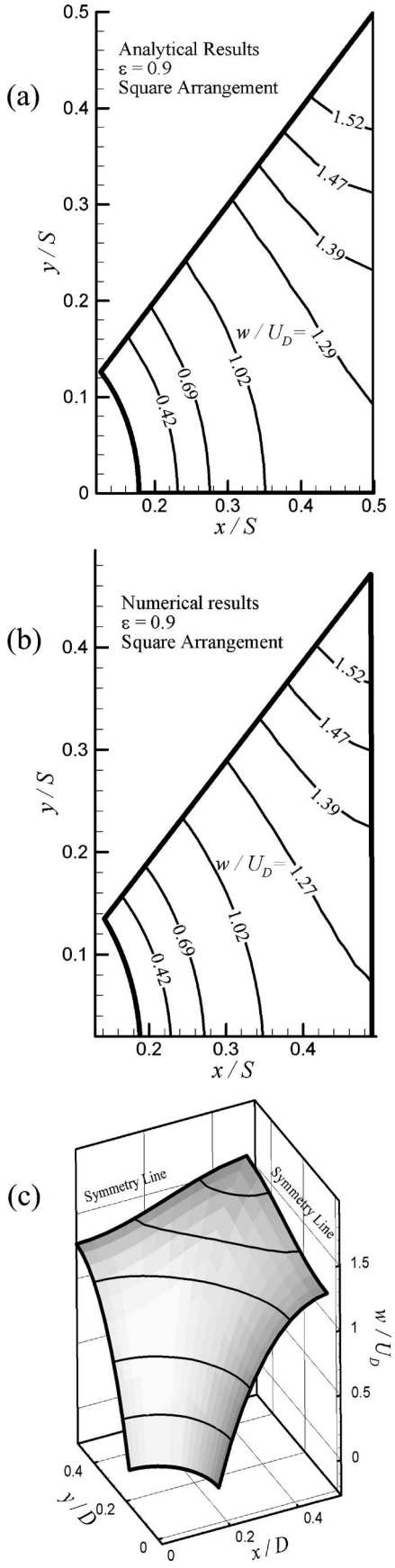

Fig. 2 (*a*) analytical velocity contours, Eq. (13), (*b*) numerical velocity contours, and (*c*) analytical velocity distribution for a square arrangement with $\varepsilon=0.9$

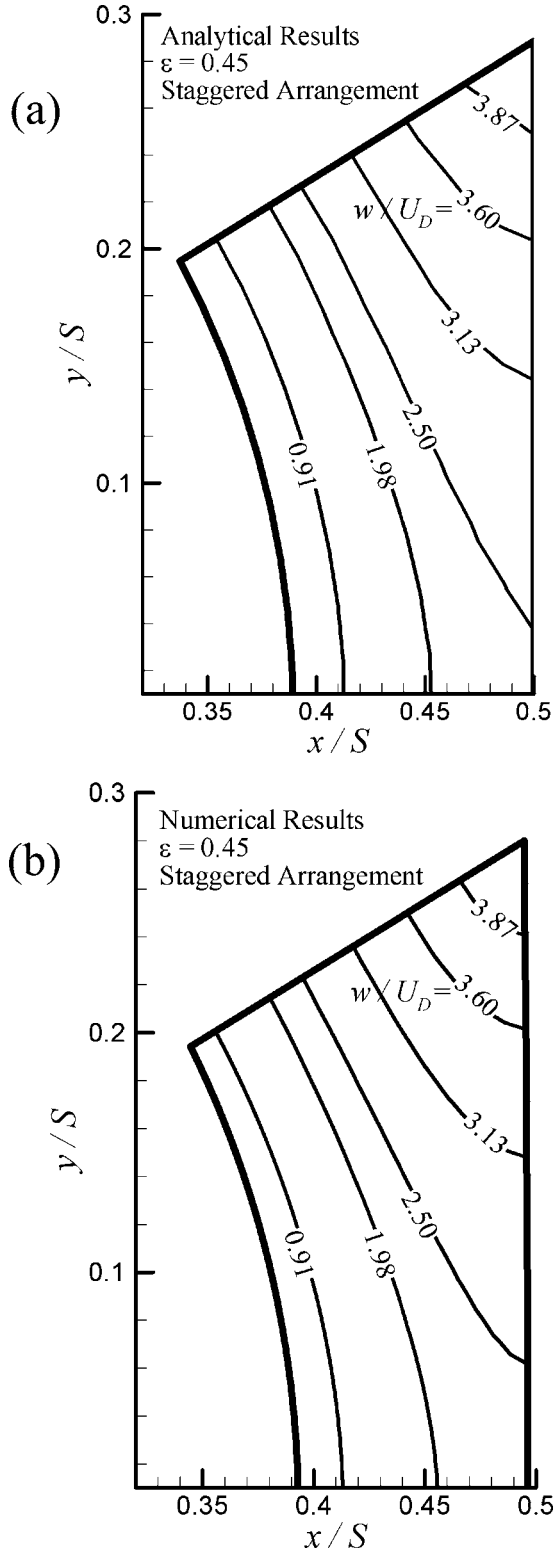

Fig. 3 Present velocity distributions for staggered arrangement of cylinders with $\varepsilon = 0.45$ (*a*) analytical, Eq. (13), and (*b*) numerical

did not provide a compact relationship for the velocity distribution.

In Fig. 6, the present model is compared with the numerical results, an experimental data reported by Farlow [27], and the models of Happel [12] and Drummond and Tahir [14]. In addition,

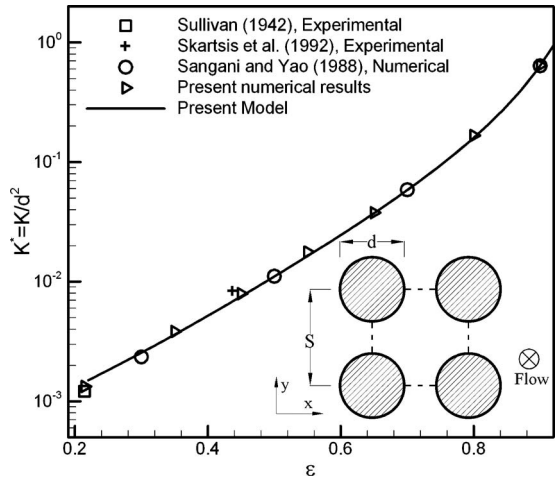

Fig. 4 Comparison of the proposed model with the numerical and experimental results; square arrangement

the permeability of touching fibers is calculated from the solution of Shit [30] for touching fibers and is included in Fig. 6. This figure shows that the present model is accurate over the entire range of porosity; especially, in lower porosities were the other models fail.

The present analytical solution, present numerical results, the models of Drummond and Tahir [14] and Happel [12] for hexagonal arrangement are compared in Fig. 7. The proposed relationship for permeability of hexagonal arrays captures the numerical results within 9% accuracy.

The relationships for dimensionless permeability of various arrangements, given in Eq. (14), are very similar to each other and the differences are in the constants and the higher order terms. The higher order terms become negligible for highly porous structures, i.e., $\varphi \to 0$. Therefore, it is expected that the three equations lead to almost identical values in this limit. As shown in Fig. 8, for $\varepsilon > 0.85$ the difference between the models is less than 5%; therefore, the permeability can be considered to be independent of microstructure. For lower porosities, on the other hand, the effect of higher order terms is considerable and the staggered array has the lowest permeability while the hexagonal arrangement is the

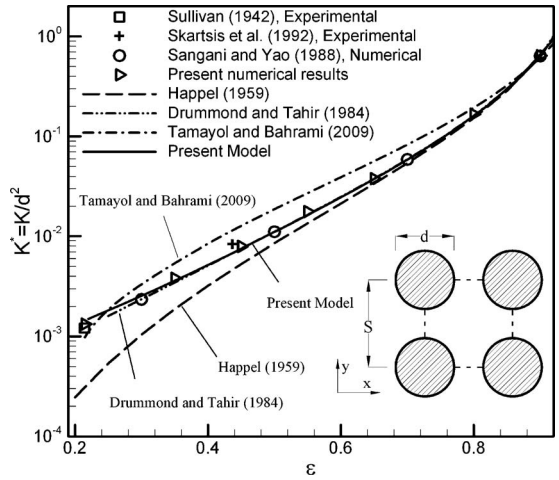

Fig. 5 Comparison of the proposed model, experimental and numerical data, and other existing models; square arrangement

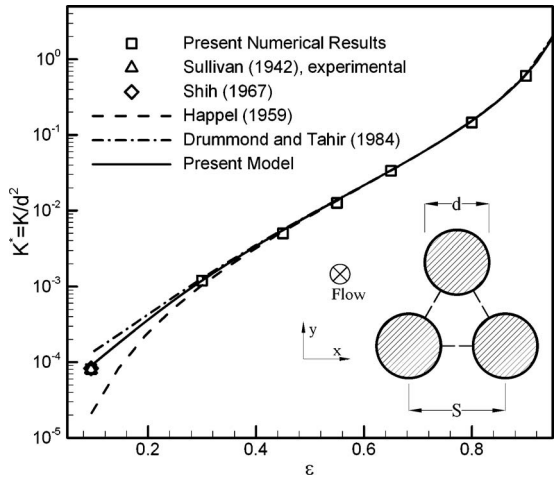

Fig. 6 Comparison of the proposed model, an experimental data point (touching limit), and other existing models; staggered arrangement

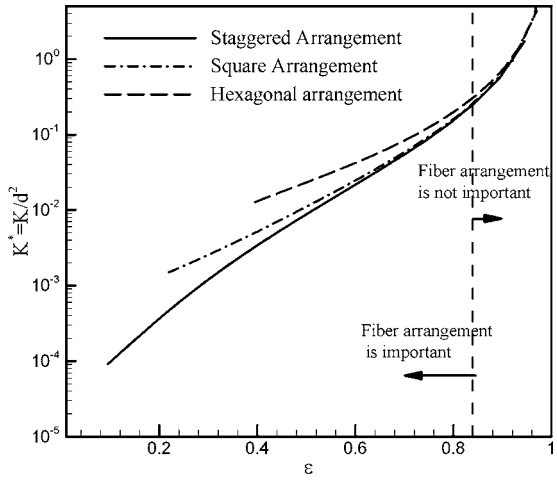

Fig. 8 Effect of arrangement on the permeability

most permeable microstructure. This is in-line with our previous observations for fully developed flow through channels with regular polygonal cross sections [31].

5 Summary and Conclusions

Fluid flow parallel to staggered, square, and hexagonal arrays of cylinders is studied both analytically and numerically. A truncated form of the series solution of Poisson's equation provides accurate results for velocity distribution in the investigated channel-like geometries. Using the proposed solutions and by neglecting higher other terms in the series solutions, compact models are developed for permeability of the media.

Independent numerical simulations are performed to verify the solutions for velocity distribution and permeability. The present approach captures the numerical results for permeability within maximum 10% accuracy for the considered arrangements, respectively. Fiber arrangement has negligible effect on the pressure drop and permeability for high porosities $\varepsilon > 0.85$. On the other hand, for lower porosities the effect of microstructure is significant and staggered arrays have lower permeability than other arrangements. As such, use of hexagonal arrays of tube in heat exchangers reduces the consequent pressure drop.

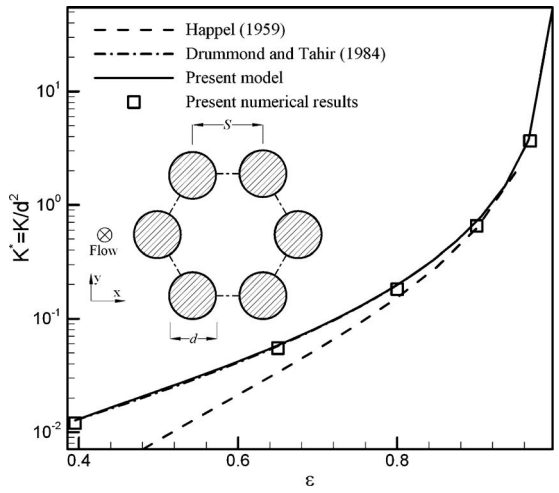

Fig. 7 Comparison of the proposed model with other existing models; hexagonal arrangement

Acknowledgment

The authors gratefully acknowledge the financial support of the Natural Sciences and Engineering Research Council of Canada (NSERC).

Nomenclature

- d = fiber diameter, m
- K = viscous permeability, m^2
- K^* = dimensionless viscous permeability, $K^*=K/d^2$
- P = pressure, Pa
- Q = volumetric flow rate, m^3/s
- r_0 = fiber radius, m
- S = distance between adjacent fibers, m
- U_D = volume-averaged superficial velocity, m/s
- w = velocity in z-direction, m/s

Greek Symbols

- ε = porosity
- μ = fluid viscosity, Ns/m^2
- φ = solid volume fraction, $\varphi=1-\varepsilon$

References

[1] Kaviany, M., 1992, *Principles of Heat Transfer in Porous Media*, Springer-Verlag, New York.

[2] Tahir, M. A., and Vahedi Tafreshi, H., 2009, "Influence of Fiber Orientation on the Transverse Permeability of Fibrous Media," Phys. Fluids, **21**, p. 083604.

[3] Calmidi, V. V., and Mahajan, R. L., 2000, "Forced Convection in High Porosity Metal Foams," ASME J. Heat Transfer, **122**, pp. 557–565.

[4] Clague, D. S., Kandhai, B. D., Zhang, R., and Sloot, P. M. A., 2000, "Hydraulic Permeability of (Un)Bounded Fibrous Media Using the Lattice Boltzmann Method," Phys. Rev. E, **61**(1), pp. 616–625.

[5] Spielman, L., and Goren, S. L., 1968, "Model for Predicting Pressure Drop and Filtration Efficiency in Fibrous Media," Environ. Sci. Technol., **2**, pp. 279–287.

[6] Jaganathan, S., Vahedi Tafreshi, H., and Pourdeyhimi, B., 2008, "A Realistic Approach for Modeling Permeability of Fibrous Media: 3-D Imaging Coupled With CFD Simulation," Chem. Eng. Sci., **63**, pp. 244–252.

[7] Zobel, S., Maze, B., Wang, Q., Vahedi Tafreshi, H., and Pourdeyhimi, B., 2007, "Simulating Permeability of 3-D Calendered Fibrous Structures," Chem. Eng. Sci., **62**, pp. 6285–6296.

[8] Gostick, J. T., Fowler, M. W., Pritzker, M. D., Ioannidis, M. A., and Behra, L. M., 2006, "In-Plane and Through-Plane Gas Permeability of Carbon Fiber Electrode Backing Layers," J. Power Sources, **162**, pp. 228–238.

[9] Tomadakis, M. M., and Robertson, T., 2005, "Viscous Permeability of Random Fiber Structures: Comparison of Electrical and Diffusion Estimates With Experimental and Analytical Results," J. Compos. Mater., **39**, pp. 163–188.

[10] Jackson, G. W., and James, D. F., 1986, "The Permeability of Fibrous Porous Media," Can. J. Chem. Eng., **64**, pp. 364–374.

[11] Happel, J., and Brenner, H., 1973, *Low Reynolds Number Hydrodynamics*, Noordhoff, Groningen.

[12] Happel, J., 1959, "Viscous Flow Relative to Arrays of Cylinders," AIChE J., **5**, pp. 174–177.

[13] Sparrow, E. M., and Loeffler, A. L., 1959, "Longitudinal Laminar Flow Between Cylinders Arranged in Regular Array," AIChE J., **5**, pp. 325–330.
[14] Drummond, J. E., and Tahir, M. I., 1984, "Laminar Viscous Flow Through Regular Arrays of Parallel Solid Cylinders," Int. J. Multiphase Flow, **10**, pp. 515–540.
[15] Astrom, B. T., Pipes, R. B., and Advani, S. G., 1992, "On Flow Through Aligned Fiber Beds and Its Application to Composite Processing," J. Compos. Mater., **26**(9), pp. 1351–1373.
[16] Wang, C. Y., 2001, "Stokes Flow Through a Rectangular Array of Circular Cylinders," Fluid Dyn. Res., **29**, pp. 65–80.
[17] Tamayol, A., and Bahrami, M., 2009, "Analytical Determination of Viscous Permeability of Fibrous Porous Media," Int. J. Heat Mass Transfer, **52**, pp. 2407–2414.
[18] Tamayol, A., and Bahrami, M., 2008, "Numerical Investigation of Flow in Fibrous Porous Media," ECI International Conference on Heat Transfer and Fluid Flow in Microscale, Whistler, Canada, Sep. 21–26.
[19] Fluent Inc., 2007, FLUENT 6.3 Users' Guide, Lebanon, USA.
[20] Jaganathan, S., Vahedi Tafreshi, H., and Pourdeyhimi, B., 2008, "On the Pressure Drop Prediction of Filter Media Composed of Fibers With Bimodal Diameter Distributions," Powder Technology, **181**, pp. 89–95.
[21] Mattern, K. J., and Deen, W. M., 2008, "Mixing Rules for Estimating the Hydraulic Permeability Of Fiber Mixtures," AIChE J., **54**, pp. 32–41.
[22] Clague, D. S., and Philips, R. J., 1997, "A Numerical Calculation of the Hydraulic Permeability of Three-Dimensional Disordered Fibrous Media," Phys. Fluids, **9**(6), pp. 1562–1572.
[23] Giuliani, J., and Vafai, K., 1999, "Particle Arrestance Modeling Within Fibrous Porous Media," ASME J. Fluids Eng., **121**, pp. 155–163.
[24] Inoue, M., and Nakayama, A., 1998, "Numerical Modeling of Non-Newtonian Fluid Flow in a Porous Medium Using a Three-Dimensional Periodic Array," ASME J. Fluids Eng., **120**, pp. 131–136.
[25] Sobera, M. P., and Kleijn, C. R., 2006, "Hydraulic Permeability of Ordered and Disordered Single-Layer Arrays of Cylinders," Phys. Rev. E, **74**, p. 036301.
[26] Higdon, J. J. L., and Ford, G. D., 1996, "Permeability of Three-Dimensional Models of Fibrous Porous Media," J. Fluid Mech., **308**, pp. 341–361.
[27] Farlow, S. J., 1993, *Partial Differential Equations for Scientists and Engineers*, Dover, New York.
[28] Sullivan, R. R., 1942, "Specific Surface Measurements on Compact Bundles of Parallel Fibers," J. Appl. Phys., **13**, pp. 725–730.
[29] Skartsis, L., Khomami, B., and Kardos, J. L., 1992, "Resin Flow Through Fiber Beds During Composite Manufacturing Processes. Part II: Numerical and Experimental Studies of Newtonian Flow Through Ideal and Actual Fiber Beds," Polym. Eng. Sci., **32**(4), pp. 231–239.
[30] Shit, F. S., 1967, "Laminar Flow in Axisymmetric Conduits by a Rational Approach," Can. J. Chem. Eng., **45**, pp. 285–294.
[31] Tamayol, A., and Bahrami, M., "Laminar Flow in Microchannels With Non-Circular Cross-Section," ASME J. Fluids Eng., accepted.